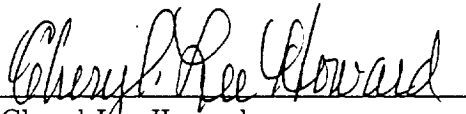


The Structure of Active Galactic Nuclei

NASA Long Term Space Astrophysics Program

Second Year Progress Report

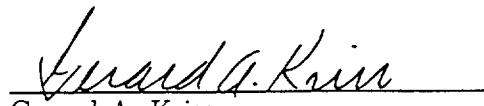
Grant NAG 5-3255


Cheryl-Lee Howard

Assistant Dean

Homewood Research Administration

The Johns Hopkins University


Gerard A. Kriss

Principal Investigator

Department of Physics & Astronomy

The Johns Hopkins University

June 18, 1997

Contents

1	Introduction	1
2	Highlights of Scientific Results in Year 2	1
2.1	Collimating the Radiation in AGN	1
2.2	Monitoring Variability in NGC 4151 during Astro-2	3
2.3	HST Observations of NGC 1068	5
2.4	Radio Observations of the Seyfert 2 Galaxy IC 5063	5
2.5	UV Diagnostic Diagrams	6
3	Publications in Year 2	8
4	References	8
5	Revised Budget and Cost Plan for Year 3	9

List of Figures

1	Representative HUT spectra of the Lyman limit region in low-redshift AGN. All spectra are shown in the object's rest frame.	2
2	HUT/Astro-2 Spectrum of NGC 4151	4
3	The variation in the neutral hydrogen column from HUT observations of NGC 4151 during Astro-2 is shown along with the continuum intensity at 1450 Å. The x-axis is in day of the year 1995. Error bars, barely visible around each data point, are 1σ .	4
4	Left: WFPC2 continuum image of NGC 1068 constructed from continuum light in the three filters F218W, F336W, and F547M. Lighter shades are higher intensity and bluer in color. Compare the blue cone of bright light to the ionization cone traced by the [O III] $\lambda 5007$ emission on the right. Right: WFPC2 image of NGC 1068 in the light of [O III] $\lambda 5007$. In both images North is up and East is to the left. Each image is $4.5''$ on each side.	6
5	Total H I intensity map of IC 5063 superimposed onto the optical image of the galaxy. The "hole" in the center of the H I distribution (and coincident with the center of the galaxy) represents the region of strong absorption against the radio continuum. Contour levels: 1.0×10^{20} to 1.72×10^{21} in steps of 1.8×10^{20} atoms cm^{-1} .	7
6	Diagnostic diagram using intensity ratios of UV carbon lines. Power-law photoionization models with spectral indices $\alpha = -1$ and $\alpha = -1.4$ have tic marks spanning ionization parameters $\log U = -1$ to $\log U = -3$. Shock+precursor models have shock velocities spanning $v = 150$ to $v = 500 \text{ km s}^{-1}$ as do the shock models with no photoionization precursor.	8

List of Tables

1	AGN with HUT Lyman Limit Observations	3
2	Budget Summary for Years 3-5	10

1 Introduction

We are continuing our systematic investigation of the nuclear structure of nearby active galactic nuclei (AGN). Upon completion, our study will characterize hypothetical constructs such as narrow-line clouds, obscuring tori, nuclear gas disks, and central black holes with physical measurements for a complete sample of nearby AGN. The major scientific goals of our program are

- the morphology of the NLR,
- the physical conditions and dynamics of individual clouds in the NLR,
- the structure and physical conditions of the warm reflecting gas,
- the structure of the obscuring torus,
- the population and morphology of nuclear disks/tori in AGN,
- the physical conditions in nuclear disks, and
- the masses of central black holes in AGN.

We will use the Hubble Space Telescope (HST) to obtain high-resolution images and spatially resolved spectra. Far-UV spectroscopy of emission and absorption in the nuclear regions using HST/FOS and the Hopkins Ultraviolet Telescope (HUT) will help establish physical conditions in the absorbing and emitting gas. By correlating the dynamics and physical conditions of the gas with the morphology revealed through our imaging program, we will be able to examine mechanisms for fueling the central engine and transporting angular momentum. The kinematics of the nuclear gas disks may enable us to measure the mass of the central black hole. Contemporaneous X-ray observations using ASCA will further constrain the ionization structure of any absorbing material. Monitoring of variability in the UV and X-ray absorption will be used to determine the location of the absorbing gas—possibly in the outflowing warm reflecting gas, or the broad-line region, or the atmosphere of the obscuring torus. Supporting ground-based observations in the optical, near-IR, imaging polarimetry, and the radio will complete our picture of the nuclear structures. With a comprehensive survey of these characteristics in a complete sample of nearby AGN, our conclusions should be more reliably extended to AGN as a class.

In this progress report we summarize highlights of our second year of study and present a bibliography of publications resulting from this year's efforts.

2 Highlights of Scientific Results in Year 2

Our principal results in this second year of investigation are based on observations obtained with the Hopkins Ultraviolet Telescope (HUT), with the Hubble Space Telescope (HST), with ground-based instruments, and on supporting theoretical work.

2.1 Collimating the Radiation in AGN

Unified models of AGN use a combination of obscuration, reflection, and orientation to explain the different appearances of Seyfert 1 and Seyfert 2 galaxies (see the review by Antonucci 1993). This picture implies some anisotropy for the escaping ionizing radiation. This has important consequences for the morphology of the NLR (Wilson 1997). If NLR gas is spherically distributed about the nuclear region, the escaping radiation will produce biconical structures projected onto the sky in obscured AGN (Type 2) and more compact, more symmetric structures in those viewed pole on (Type 1's). By and large, this is what is observed (e.g., Pogge 1989; Evans et al. 1994).

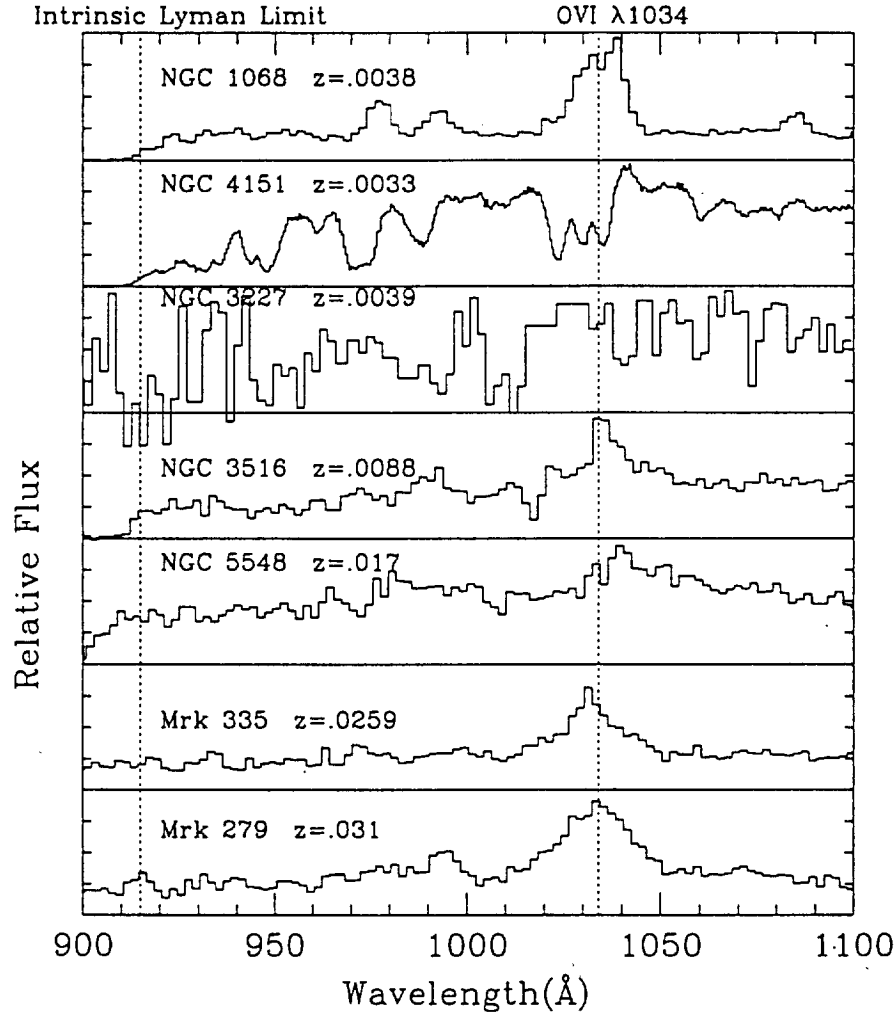


Figure 1: Representative HUT spectra of the Lyman limit region in low-redshift AGN. All spectra are shown in the object's rest frame.

In more general terms, one could classify the means of collimating the ionizing radiation in one of two categories: intrinsic anisotropy, or geometrical shadowing. Examples of intrinsically anisotropic radiation would be that due to relativistic beaming or the radiation from an accretion funnel in a geometrically thick accretion disk. Geometrical shadows that collimate the radiation can be produced not only by the obscuring torus, but also by the wind from an accretion disk or by a toroidal configuration of broad-line region clouds. *All examples of shadowing predict we should see optically thick neutral hydrogen absorption at the Lyman limit.*

Of 13 AGN with $z < 0.3$ observed with HUT, only 4 show intrinsic Lyman limits. Table 1 summarizes the HUT Astro-1 and Astro-2 observations, and Figure 1 shows representative spectra. All objects with Lyman limit absorption (NGC 1068, NGC 4151, NGC 3516, and NGC 3227) have narrow-line regions with bipolar morphologies. The remaining 9 AGN are Seyfert 1's or low-redshift quasars with point-like NLR's as imaged with HST or from the ground. *Seeing absorption only in objects with bipolar NLR's favors shadowing for collimation over an intrinsically beamed mechanism.*

Table 1: AGN with HUT Lyman Limit Observations

Object	Type	z	NLR Morphology	Lyman Limit?
NGC 1068	2	0.0038	bi-cone	yes
NGC 4151	1	0.0033	bi-cone	yes
NGC 3227	1	0.0039	bi-cone	yes (95% confidence)
NGC 3516	1	0.0088	S-shape	yes
NGC 5548	1	0.017	point-like	no
Mrk 335	1	0.026	point-like	no
Mrk 279	1	0.031	point-like	no
Mrk 509	1	0.035	point-like	no
Mrk 478	1	0.077	point-like	no
PG1211+143	1	0.081	?	no
PG1351+640	1	0.088	?	no
3C 273	1	0.158	jet	no
E1821+64	1	0.297	point-like	no

2.2 Monitoring Variability in NGC 4151 during Astro-2

Monitoring variability in absorption features allows one to pinpoint the location of the absorbing gas. We observed NGC 4151 on six separate occasions at intervals of one to three days using the Hopkins Ultraviolet Telescope during the flight of Astro-2 aboard the space shuttle *Endeavour* in March 1995. The far-ultraviolet spectra cover the spectral range from the interstellar cutoff at 912 Å to 1840 Å with a resolution of 2–4 Å. The mean spectrum, shown in Figure 2, represents 4752 s of integration time, with a mean S/N of ~ 30 . It shows profound differences (Kriss et al. 1995) compared to the one obtained during the flight of Astro-1 in December 1990 (Kriss et al. 1992).

Our absorption line variability measurements allow us to measure two timescales—the ionization timescale and the recombination timescale—each of which allows some measure of the distance of the absorbing gas from the central source. The data shown in Figure 3 exhibit an approximate δ -function blip in the continuum flux and the change of the neutral hydrogen column in response. When the continuum flux rises (a 60% increase, or $\Delta L = 1.4 \times 10^{43}$ erg s $^{-1}$), we see a nearly instantaneous drop in the neutral hydrogen column ($\Delta N_{HI} = 7.5 \times 10^{17}$ cm $^{-2}$) giving an ionization timescale of < 2 days, the limit of our sampling. After the continuum returns to its mean intensity, the neutral hydrogen column gradually increases with an e-folding timescale of ~ 10 days.

The decrease in the neutral hydrogen column, ΔN_{HI} , and the time, Δt , required to respond to the continuum increase, ΔL , provide a direct measure of the number of ionizing photons and indirectly give a measure of the distance of the absorber from the source. Since

$$\Delta N_{HI} = (\# \text{ ionizing photons}) / (4\pi r^2), \text{ and}$$

$$\Delta L = (\# \text{ ionizing photons}) \times h\nu / \Delta t,$$

the distance of the absorber from the source can be found as

$$r = [(\Delta L \Delta t) / (4\pi \Delta N_{HI} h\nu)]^{1/2}.$$

For our observations of NGC 4151, an upper limit of 2 days on the ionization timescale translates into an upper limit of 30 pc on the radius of the absorbing gas.

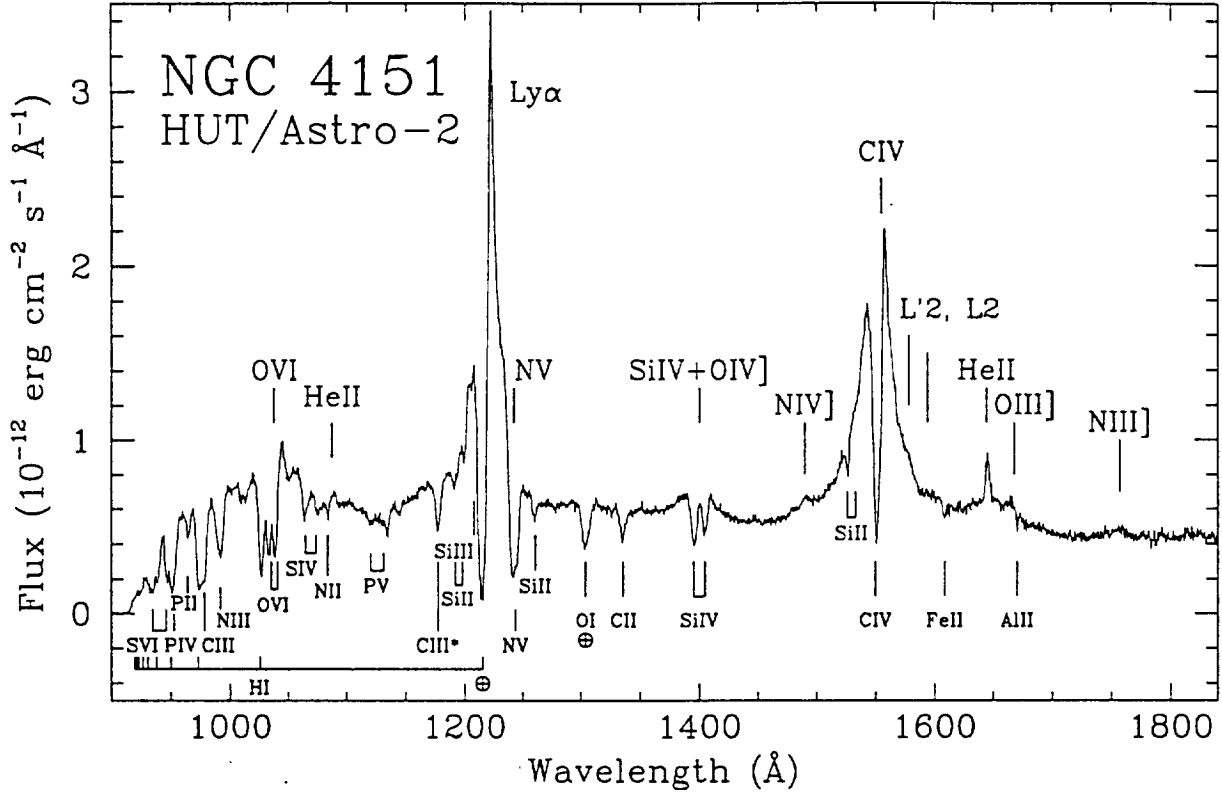


Figure 2: The flux-calibrated mean spectrum of NGC 4151 obtained with the Hopkins Ultraviolet Telescope during the Astro-2 mission is shown. Prominent emission and absorption lines are marked. The earth symbol indicates features affected by geocoronal Ly α and O I emission.

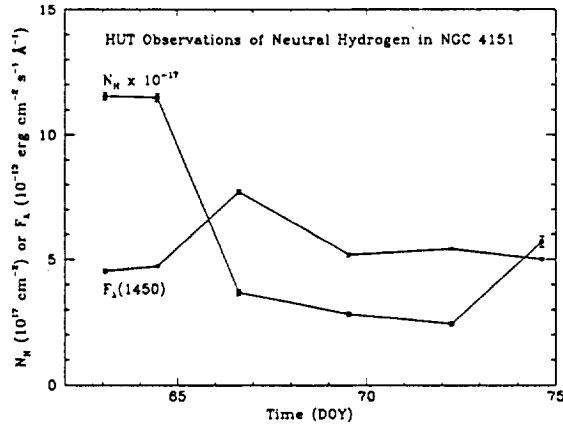


Figure 3: The variation in the neutral hydrogen column from HUT observations of NGC 4151 during Astro-2 is shown along with the continuum intensity at 1450 Å. The x-axis is in day of the year 1995. Error bars, barely visible around each data point, are 1σ .

The recombination timescale, $t_{rec} = (1/n_e \alpha_{rec})(n_{HI}/n_{HII})$, is often cited as a measure of the density of absorbing material, but this is true only if one knows the ionization state of the gas (Krolik & Kriss 1995). The neutral fraction n_{HI}/n_{HII} depends on the ionization parameter $U = L/(4\pi r^2 h \nu (n_e + n_p))$ as $n_{HI}/n_{HII} = Q/U$, where Q is typically $\sim 4.5 \times 10^{-6}$, determined by atomic data and the shape of the ionizing spectrum. These relations can be used to obtain a

distance estimate for the gas based on the observed recombination time:

$$r = 62 \text{ pc} \left(\frac{\Delta t}{10 \text{ d}} \right)^{1/2} \left(\frac{L}{2.3 \times 10^{43} \text{ erg s}^{-1}} \right)^{1/2} \left(\frac{15,000 \text{ K}}{T} \right)^{0.4} \left(\frac{4.5 \times 10^{-6}}{Q} \right)^{1/2}.$$

For our observations of NGC 4151, the absorbing gas is located far from the central source in the NLR. The absorbing gas may be outflowing material driven off the surface of the obscuring torus.

2.3 HST Observations of NGC 1068

We have analyzed the large set of WFPC2 images of NGC1068 taken as part of the FOS GTO program. The database covers the wavelength range from 2000–9000 Å and includes images in several emission lines ([Ne v] λ3426, [O II] λ3727, [O III] λ5007, Hα+[N II]) and continuum bands (F218W, F336W, F547M, F791W). This data set was used to map the morphology of the emitting gas in both low- and high-ionization lines as well as the morphology of the UV continuum radiation and to compare these with the distribution of obscuring material revealed by the reddening map. The major results of our study can be summarized as follows:

- A cone of UV continuum light is well outlined in the combined continuum maps basically coincident with the emission line ionization cone known from previous ground-based and HST imaging. Figure 4 compares the continuum light distribution with that of [O III] λ5007.
- Emission line and UV cones have the same opening angle ($\Theta \sim 80^\circ$) and orientation.
- There is a signature of an obscuring formation (disk, torus ??) with size $d \sim 0.5''$ (50 pc) oriented roughly E-W, i.e., approximately perpendicular to the projected position of the inner radio jet.
- Emission line ratio maps suggest that there could be self shielding in some directions within the ionization cone.

2.4 Radio Observations of the Seyfert 2 Galaxy IC 5063

New radio continuum (8 GHz and 1.4 GHz) and H I 21 cm line observations of the Seyfert 2 galaxy IC 5063 (PKS 2048-572) were obtained with the Australia Telescope Compact Array (ATCA). The high resolution 8 GHz image shows a linear triple structure of $\sim 4''$ (1.5 kpc) in size. This small-scale radio emission shows a strong morphological association with the inner part of the optical emission line region (NLR). It is aligned with the inner dust lane and is oriented perpendicular to the position angle of the optical polarization. We identify the radio nucleus to be the central blob of the radio emission. At 21 cm, very broad ($\sim 700 \text{ km s}^{-1}$) H I absorption is observed against the strong continuum source. This absorption is almost entirely blueshifted, indicating a fast net outflow, but a faint and narrow redshifted component is also present. In IC 5063 we see clear evidence, both morphological and kinematical, for strong shocks resulting from the interaction between the radio plasma and the interstellar medium in the central few kiloparsecs. However, we estimate the energy flux in the radio plasma to be an order of magnitude smaller than the energy flux emitted in emission lines, so the shocks associated with the jet-ISM interaction are unlikely to account for the ionization of the NLR.

The main structure of the H I emission is a warped disk associated with the system of dust lanes of $\sim 2'$ radius ($\sim 38 \text{ kpc}$, corresponding to ~ 5 effective radii). H I contours are superposed

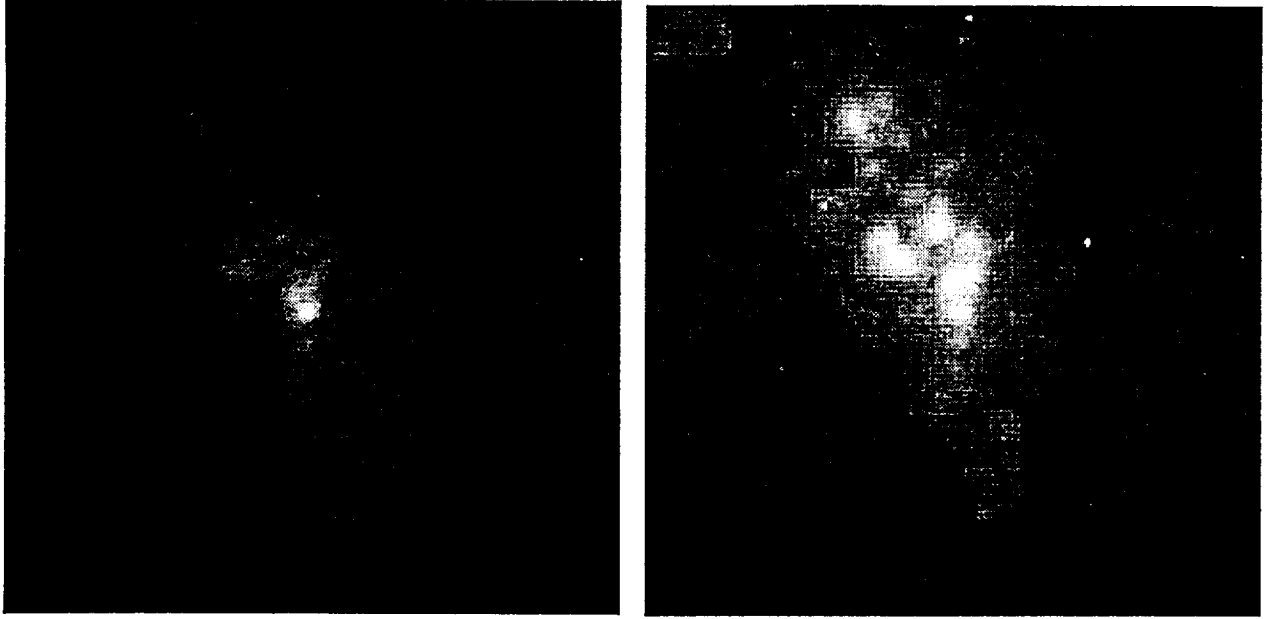


Figure 4: **Left:** WFPC2 continuum image of NGC 1068 constructed from continuum light in the three filters F218W, F336W, and F547M. Lighter shades are higher intensity and bluer in color. Compare the blue cone of bright light to the ionization cone traced by the $[\text{O III}] \lambda 5007$ emission on the right. **Right:** WFPC2 image of NGC 1068 in the light of $[\text{O III}] \lambda 5007$. In both images North is up and East is to the left. Each image is $4.5''$ on each side.

on an optical image of IC 5063 in Figure 5. The lack of kinematically disturbed gas (both neutral and ionized) outside the central few kpc, the warped structure of the large scale disk together with the close morphological connection between the inner dust lanes and the large-scale ionized gas, support the idea that the gas at large radii is photoionized by the central region, while shadowing effects are important in defining its X-shaped morphology.

From the kinematics of the ionized and of the neutral gas, we find evidence for a dark halo in IC 5063, with very similar properties as observed in some other early-type galaxies.

2.5 UV Diagnostic Diagrams

Identifying the principal ionization mechanism in the emission line regions of AGN is of main importance in studying the physics of transporting the energy from the central engine to the ISM in the host galaxy and beyond. Traditionally, attempts to distinguish between different excitation mechanisms in active galaxies have relied on observations of emission lines at optical wavelengths. These tests have been unable to provide conclusive discrimination between the competing mechanisms because both shocks and photoionization can reproduce most of the observed optical line ratios. However, the intensities of the UV lines are predicted to be much stronger in shocks than in simple photoionized plasma. The large differences in the rates of collisional excitation of these UV lines therefore provides a potential means to discriminate between the models.

Through careful analysis of the predictions of the photoionization and shock models we have identified a set of UV only and UV-optical line ratio diagrams which can discriminate between pure shock and photoionization modes of excitation, and to a large extent, also discriminate shocks with ionized precursors from photoionization. These diagrams use relatively bright emission lines

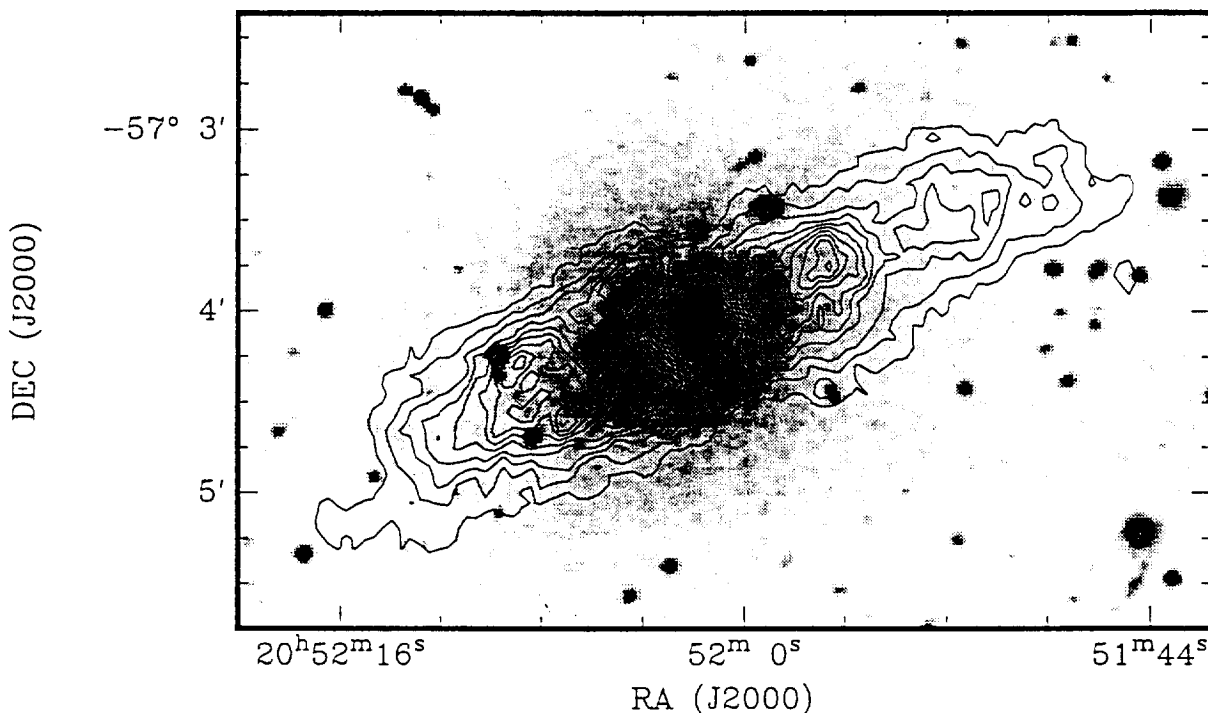


Figure 5: Total H I intensity map of IC 5063 superimposed onto the optical image of the galaxy. The “hole” in the center of the H I distribution (and coincident with the center of the galaxy) represents the region of strong absorption against the radio continuum. Contour levels: 1.0×10^{20} to 1.72×10^{21} in steps of 1.8×10^{20} atoms cm^{-1} .

and reddening insensitive ratios and provide a practical observational test for separating the excitation mechanisms of the narrow line regions of active galaxies. In general, the diagrams show that we can, to a large extent, separate photoionization from shocks with precursors if the shock velocity is less than 400 km s^{-1} . Above 400 km s^{-1} the shock+precursor grids overlap with the photoionization models. The most useful diagnostics utilize the (C II] $\lambda 2326$ /C III] $\lambda 1909$), (C IV $\lambda 1549$ /C III] $\lambda 1909$) ratio pair. These diagnostics are illustrated in Figure 6. The near-UV ([Ne V] $\lambda 3426$ /[Ne III] $\lambda 3869$) ratio also provides a good diagnostic that can be easily measured with ground based instruments. These UV diagnostics are expected to form a useful observational tool for comparison with UV spectra obtained with the FOS and particularly for spatially mapped UV spectra that will be obtained with STIS. We also have demonstrated that the FUV lines C III $\lambda 977$ and N III $\lambda 991$ are sensitive temperature diagnostics which can discriminate between the models.

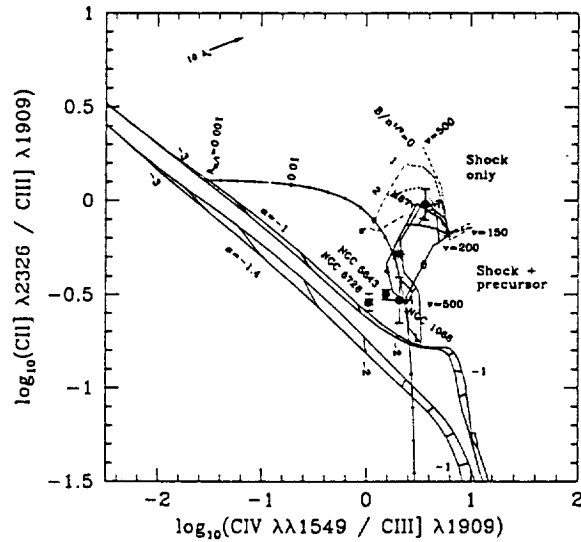


Figure 6: Diagnostic diagram using intensity ratios of UV carbon lines. Power-law photoionization models with spectral indices $\alpha = -1$ and $\alpha = -1.4$ have tic marks spanning ionization parameters $\log U = -1$ to $\log U = -3$. Shock+precursor models have shock velocities spanning $v = 150$ to $v = 500 \text{ km s}^{-1}$ as do the shock models with no photoionization precursor.

3 Publications in Year 2

1. "UV Diagnostics for the Emission Line Gas in Active Galaxies", Allen, M.G., Dopita, M.A., & Tsvetanov, Z.I. 1997, ApJ, submitted
2. "HUT Observations of the Lyman Limit in AGN: Implications for Unified Models", Kriss, G., Krolik, J., Grimes, J., Tsvetanov, Z., Zheng, W., & Davidsen, A. 1996, in proc. IAU Colloquium 159, *Emission Lines in Active Galaxies: New Methods and Techniques*, eds. B.M. Peterson, F.-Z. Cheng, & A.S. Wilson (Astronomical Society of the Pacific: San Francisco), 113, 453
3. "Resolving the C IV and Mg II Absorption in NGC 4151", Kriss, G. A. 1997, in Proceedings of the GHRS Science Symposium, September 1996, eds. J.C. Brandt, C.C. Petersen, and T.B. Ake, (Astronomical Society of the Pacific: San Francisco), in press
4. "A Radio Study of the Seyfert Galaxy IC 5063", Morganti, R., Oosterloo, T., & Tsvetanov, Z. 1997, AJ, submitted.

4 References

- Antonucci, R. 1993, ARAA, 31, 473
 Evans et al. 1994, ASP Conf. Ser., 54, 3
 Kriss, G. A., Davidsen, A. F., Zheng, W., Kruk, J. W., & Espey, B. R. 1995, ApJ, 454, L7
 Kriss, G. A., et al. 1992, ApJ, 392, 485
 Krolik, J. H., & Kriss, G. A. 1995, ApJ, 447, 512
 Pogge, R. 1989, ApJ, 345, 730
 Wilson, A. S. 1997, ASP Conf. Ser., 113, p. 264

5 Revised Budget and Cost Plan for Year 3

The peer review committee recommended personnel support as described below with a funding level of \$78,000 for the third year of our program. Drs. Kriss and Tsvetanov are funded at a level of two months per year for the life of the project, and Dr. Zheng is funded at 1 month per year. The senior investigators, Drs. Ford and Davidsen, are not funded. JHU projects a personnel benefit rate of 28% for staff in UFY '97 (7/1/96-6/30/97) and in UFY '98. A detailed breakdown of the individual entries in our budget summary is described here and in the accompanying table.

Consistent with the funding recommendations of the peer review, our travel costs include one observing trip per year each to Arizona and to Chile, one trip per year to an AAS meeting, and one trip per year to an international conference. For each five-day observing trip in Arizona we estimate costs at \$964 for round trip airfare, \$60/day lodging, and \$40/day meals and miscellaneous expenses. For each seven-day trip to Chile we estimate round-trip air fare at \$1850 and meals and lodging at \$100/day. For each five-day AAS trip we estimate costs at \$750 for round trip airfare, \$150 registration, \$80/day lodging, and \$40/day meals and miscellaneous expenses. For trips to an international conference we estimate seven-day trips with \$1,500 for round-trip air fare and \$200/day for meals and lodging.

Supplies and materials are the normal office type expended in this type of program, including magnetic tapes for data backup and storage, paper and toner for photocopying and laser printer output, and reference materials.

The Johns Hopkins Department of Physics and Astronomy has established a computing center with file servers to serve as boot nodes for workstations, to supply peripherals such as magnetic tape drives and laser printers, to negotiate group maintenance contracts, and to provide the services of a systems manager. Large software packages and software libraries such as IRAF are maintained on the file server. The center also maintains the network throughout the department. To partially defray the costs of providing these services, individual workstations are charged a monthly fee for access to the department network. This is anticipated to be \$15/month for UFY '97. Users are also charged a flat monthly fee of \$15/month for account maintenance. Hardware maintenance fees are \$73.63/month under the group contract with Sun Microsystems, and the annual software maintenance fee is \$150 for each operating system. During each year of the project we have charged these fees in direct proportion to the man-months of effort devoted to our study.

Publication costs cover the charges to print the results in *The Astrophysical Journal* and to distribute preprints. We include funds for three ApJ Letters in the third year, and two 10-page ApJ articles. Preprint costs are estimated at \$150/letter and \$250 per paper.

For UFY 1997 Johns Hopkins University has negotiated an IDC rate of 68%. For UFY 1998 it is 64.5%. For UFY 1999 and later, it is 62%. The program will be charged the applicable rates in effect in later years. All numbers after 1997 are estimates, based on an annual inflation rate of 3%.

NASA PROPOSAL BUDGET FORM LONG-TERM SPACE ASTROPHYSICS PROGRAM

Principal Investigator		Institution		Proposal Title					
Gerard A. Kriss		The Johns Hopkins University		The Structure of Active Galactic Nuclei					
A. Salaries, Senior Personnel		Monthly or Hourly Rate	No. of Months	Funds Grant Year 1	Funds Grant Year 2	Funds Grant Year 3	Funds Grant Year 4	Funds Grant Year 5	
1. PI Dr. Gerard A. Kriss		\$6,083.33	2/year			12,167	12,532	12,908	
2. Co-I Dr. Zlatan Tsvetanov		\$4,833.33	2/year			9,667	9,957	10,255	
3. Co-I Dr. Wei Zheng		\$5,000.00	1/year			5,000	5,150	5,305	
B. Salaries or Wages, Other Personnel (show numbers in parentheses)									
1. () Post Doctoral Associates									
2. () Other Professionals (Technicians, Programmers, etc.)									
3. () Administrative									
4. () Other (specify)									
C. Fringe Benefits (if charged as direct costs; specify)						7,513	7,739	7,971	
28% for staff, charged as direct cost						\$34,347	\$35,377	\$36,439	
Total Salaries, Wages, and Fringe Benefits (A+B+C)									
D. Permanent Equipment, incl. Workstation (list each item > \$5000; continue on separate sheet if necessary)									
Total Permanent Equipment			No IDC						
E. Travel, Domestic (incl. Canada, U.S. Possessions)						3,145	3,239	3,336	
Travel, Foreign						3,077	5,955	6,134	
F. Other Direct Cost									
1. Materials and Supplies (includes charges for preprints)						1,633	1,307	1,395	
2. Publication Costs (rate/page x no. of pages) \$134/pg-ApJ, \$149/pg-ApJ Ltr						4,468	3,396	3,932	
3. Computer Services - \$73.63/mo-hdwr(5), \$150/yr-sltwr(5), \$15/mo-nlwk, \$15/mo-user acct						581	598	616	
4. Subgrants/Contracts (specify) N/A									
5. Other (specify)									
G. Total Direct Cost (A through F)						\$47,249	\$49,872	\$51,852	
H. Indirect Costs (specify)									
effective 7/1/97 - 64.5%; effective 7/1/98						30,751	31,128	32,148	
I. Total (G+H)						\$78,000	\$81,000	\$84,000	
PI (signature) Gerard A. Kriss									
Cognizant Institutional Officer (type name and signature)									
Cheryl-Lee Howard									
Position/Title		Assistant Dean for Research Administration							
Address and Tel. No. of Institution's Sponsored Research Office:		Homewood Research Administration, 105 Ames Hall 3400 North Charles Street Baltimore, MD 21218 410/516-8668 Fax: 410/516-7775							

Funding begins on May 1st of each grant year

If more space is needed, please continue on back of this form or use separate sheet.

The Structure of Active Galactic Nuclei

LTSAP Proposal, G. Kriss, P.I.	inflation	5/95-4/96	5/96-4/97	5/97-4/98	5/98-4/99	5/99-4/00	TOTAL
Personnel	3%						
Dr. G. Kriss	2.0			12167	12532	12908	60503
Dr. Z. Tsvetanov	2.0			9667	9957	10255	46282
Dr. W. Zheng	1.0			5000	5150	5305	23198
Secretary	0.0			0	0	0	4544
Total Salaries				26,833	27,638	28,468	134,527
Benefits	28.0%			7,513	7,739	7,971	38,078
Total Benefits				7,513	7,739	7,971	38,078
Travel - AAS mtgs, 1/year				1,591	1,639	1,688	9,472
- Observing - Tucson, 1/year				1,553	1,600	1,648	6,265
- Observing - Chile, 1/year				0	2,786	2,870	13,821
- Intl conference - 1/year				3,077	3,169	3,264	12,409
Computer support				581	598	616	1,795
Page Charges ApJ Ltrs & ApJ				4,468	3,396	3,932	13,996
Preprint charges \$150/Ltr, 250 ApJ				950	700	700	2,900
Supplies & Materials				683	607	695	2,199
Total costs subj to IDC				47,249	49,872	51,852	235,460
Indirect cost rate effective 7/1/96	68.0%			5,355			
Indirect cost rate effective 7/1/97	64.5%			25,396	5,361		
Indirect cost rate effective 7/1/98	62.0%				25,767	32,148	
Total Indirect Costs				30,751	31,128	32,148	152,572
Maint. on Sun Wkstn @ \$73.63/mo							788
Software maintenance @ \$150/year							1,015
Network connection fee @ \$15/mo							183
User account fee @ \$15/mo							183
TOTAL COSTS				\$78,000	\$81,000	\$84,000	\$390,200
Awarded amounts:		\$72,500	\$74,700	\$78,000	\$81,000	\$84,000	\$390,200
		\$0	\$0	\$0	\$0	\$0	\$0

AAS mtg travel - Locations TBD	5/95-4/96	5/96-4/97	5/97-4/98	5/98-4/99	5/99-4/00	CATEGORY TOTAL
days	trips per year					
5			1	1	1	
Airfare	750					
Hotel, Meals, etc. @ \$120/day	600					
Registration	150					
Total for each trip	1500					
Total for AAS meeting			1591	1639	1688	7964
Observing at KPNO, AZ	trips per year					
5 days per trip			1	1	1	
Airfare	964					
Meals, Lodging, etc @ \$100/day	500					
Total for each trip	1464					
Total for KPNO Observing			1553	1600	1648	7773
Observing in Chile	trips per year					
7 days per trip			0	1	1	
Airfare	1850					
Meals, Lodging, etc @ \$100/day	700					
Total for each trip	2550					
Total for Chile Observing			0	2786	2870	10833
International Conference	trips per year					
7 days per trip			1	1	1	
Airfare	1500					
Meals, Lodging, etc @ \$200/day	1400					
Total for each trip	2900					
Total for Intl Conference			3077	3169	3264	15396
Materials & Supplies			683	607	695	2187
Preprint Costs	cost/ppr					
(charges included with Materials and Supplies, for print, copying, postage)	ApJ Ltr 150					
	Ap J 250		950	700	700	3200

Publication Costs	5/95-4/96 papers per year	5/96-4/97	5/97-4/98	5/98-4/99	5/99-4/00	
Astrophysical Journal Ltrs (4 pg) ApJ 8pg/yr1; 7pg/yr2; 10pg/yr3 & 12pg/yr4; 16pg/yr5	cost/pg 149		3	3	3	7716
Astrophysical Journal	cost/pg 134		2	1	1	8414
Total Publication costs			2680	1608	2144	16130
			4468	3396	3932	
Computer Services						
Hardware maintenance Sun Wkstns			5			
Hdw&softwr maint for all wkstns	cost/mo 73.63		368	379	391	1925
Software maintenance	cost/yr 150		63	64	66	1308
Network Connection Fee	cost/mo 15		75	77	80	415
User account fee	cost/mo 15		75	77	80	415
Total Computer Service Charges			581	598	616	3963

The Structure of Active Galactic Nuclei

NASA Long Term Space Astrophysics Program

First Year Progress Report

Grant NAGW-4443

Gerard A. Kriss
Principle Investigator
Department of Physics & Astronomy
The Johns Hopkins University
February 23, 1996

Contents

1	Introduction	1
2	Highlights of Scientific Results in Year 1	1
2.1	HUT Observations of NGC 4151 during Astro-2	1
2.2	Simultaneous HUT and ASCA Observations of NGC 3516	2
2.3	Small-Aperture Spectroscopy of the Gas Disk in M87	6
2.4	Radio Observations of Southern Seyfert Galaxies	7
3	Proposals Submitted and Approved during the First Year	9
4	Outlook for the Upcoming Year	9
5	Publications in Year 1	10
6	References	11
7	Revised Budget and Cost Plan for Year 2	12

List of Figures

1	HUT/Astro-2 Spectrum of NGC 4151	2
2	HUT/Astro-2 Spectrum of NGC 3516	3
3	ASCA X-ray Spectrum of NGC 3516	4
4	Curves of Growth for UV Absorption Lines in NGC 3516	5
5	FOS Aperture Positions in the Nucleus of M87	6
6	Rotational Velocities in the Ionized Gas Disk of M87	7
7	Radio and O III λ 5007 Emission in ESO 137-G34 and PKS 2048-57 (IC 5063) . . .	8

1 Introduction

We have begun a systematic investigation of the nuclear structure of nearby active galactic nuclei (AGN). Upon completion, our study will characterize hypothetical constructs such as narrow-line clouds, obscuring tori, nuclear gas disks, and central black holes with physical measurements for a complete sample of nearby AGN. The major scientific goals of our program are

- the morphology of the NLR,
- the physical conditions and dynamics of individual clouds in the NLR,
- the structure and physical conditions of the warm reflecting gas,
- the structure of the obscuring torus,
- the population and morphology of nuclear disks/tori in AGN,
- the physical conditions in nuclear disks, and
- the masses of central black holes in AGN.

We will use the Hubble Space Telescope (HST) to obtain high-resolution images and spatially resolved spectra. Far-UV spectroscopy of emission and absorption in the nuclear regions using HST/FOS and the Hopkins Ultraviolet Telescope (HUT) will help establish physical conditions in the absorbing and emitting gas. By correlating the dynamics and physical conditions of the gas with the morphology revealed through our imaging program, we will be able to examine mechanisms for fueling the central engine and transporting angular momentum. The kinematics of the nuclear gas disks may enable us to measure the mass of the central black hole. Contemporaneous X-ray observations using ASCA will further constrain the ionization structure of any absorbing material. Monitoring of variability in the UV and X-ray absorption will be used to determine the location of the absorbing gas—possibly in the outflowing warm reflecting gas, or the broad-line region, or the atmosphere of the obscuring torus. Supporting ground-based observations in the optical, near-IR, imaging polarimetry, and the radio will complete our picture of the nuclear structures. With a comprehensive survey of these characteristics in a complete sample of nearby AGN, our conclusions should be more reliably extended to AGN as a class.

In this progress report we will first summarize our proposed goals for this first (As yet incomplete) year of study, and then give an overview of the highlights of our first year's investigations. We will then describe a number of proposals submitted and accepted during this first year which will lay the ground work for our continuing work in the second year. Finally, we present a bibliography of publications resulting from this year's efforts.

2 Highlights of Scientific Results in Year 1

Our principle results in this first year of investigation are based on the extremely successful flight of the Hopkins Ultraviolet Telescope aboard the space shuttle *Endeavour* during the record-setting 16-day Astro-2 mission in March 1995 as well as a successful re-observation of the nuclear gas disk around the central black hole in M87.

2.1 HUT Observations of NGC 4151 during Astro-2

We observed NGC 4151 on six separate occasions at intervals of one to three days using the Hopkins Ultraviolet Telescope during the flight of Astro-2 aboard the space shuttle *Endeavour* in March 1995. The far-ultraviolet spectra cover the spectral range from the interstellar cutoff at 912 Å to 1840 Å with a resolution of 2–4 Å. The mean spectrum, shown in Figure 1, represents 4752

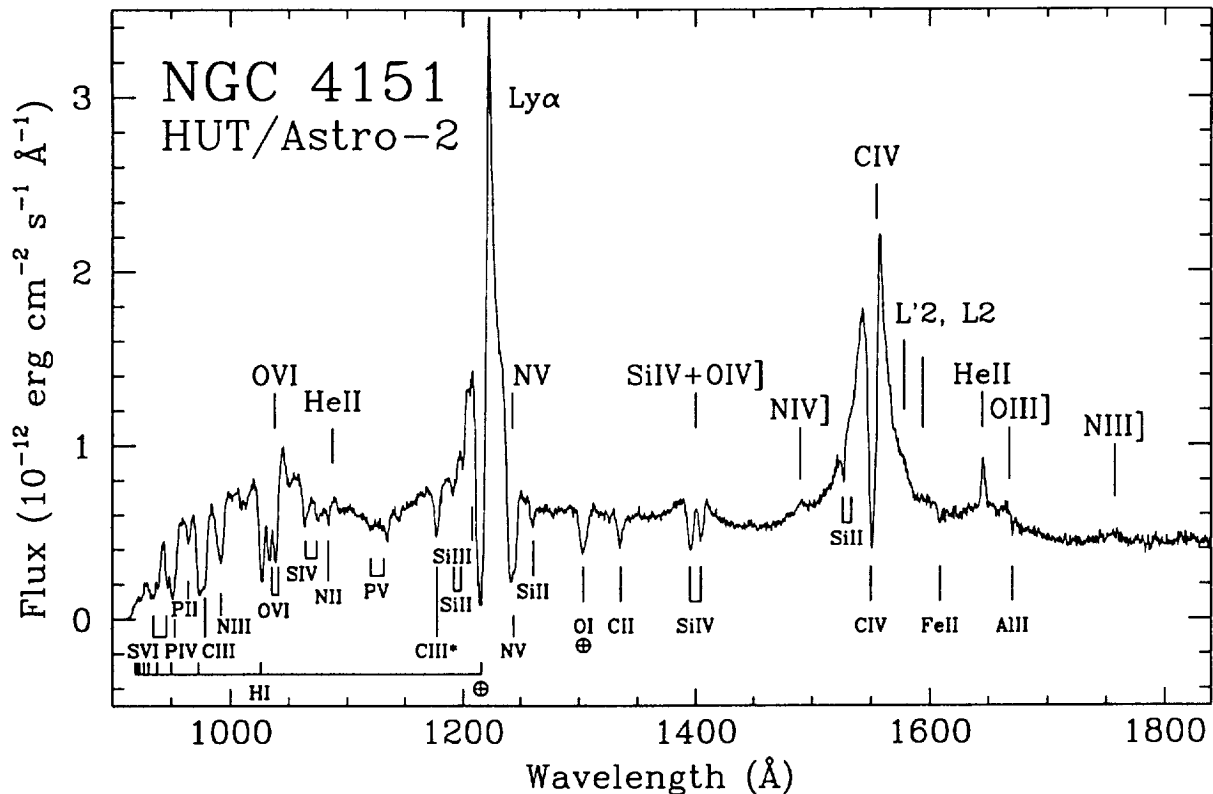


Figure 1: The flux-calibrated mean spectrum of NGC 4151 obtained with the Hopkins Ultraviolet Telescope during the Astro-2 mission is shown. Prominent emission and absorption lines are marked. The earth symbol indicates features affected by geocoronal Ly α and O I emission.

s of integration time, with a mean S/N of ~ 30 . It shows profound differences compared to the one obtained during the flight of Astro-1 in December 1990 (Kriss et al. 1992). The continuum, $5.3 \times 10^{-13} \text{ erg cm}^{-2} \text{ s}^{-1} \text{ Å}^{-1}$ at 1455 Å, is five times brighter, the brightest UV flux ever observed for NGC 4151. All high-ionization absorption lines have strengthened considerably — S VI $\lambda\lambda 933, 945$, C III $\lambda 977$, O VI $\lambda\lambda 1032, 1038$, N V $\lambda\lambda 1239, 1243$, Si IV $\lambda\lambda 1394, 1403$, and C IV $\lambda\lambda 1548, 1551$. The Lyman series absorption lines have also increased in strength, with the bulk of the absorption requiring a neutral hydrogen column density of $5 \times 10^{17} \text{ cm}^{-2}$ covering only 78% of the UV source with an effective Doppler parameter of 350 km s^{-1} . However, up to $5 \times 10^{20} \text{ cm}^{-2}$ of neutral hydrogen that fully covers the source could be present in gas with a thermal Doppler parameter of 20 km s^{-1} . Single-zone photoionization models of warm absorbing gas are unable to account for both the X-ray absorbing material and the UV-absorbing gas, largely because of the wide range of ionization states present in the UV and the X-ray.

2.2 Simultaneous HUT and ASCA Observations of NGC 3516

We observed the Seyfert 1 galaxy NGC 3516 twice during the flight of Astro-2 using the Hopkins Ultraviolet Telescope aboard the space shuttle *Endeavour* in March 1995. Simultaneous X-ray observations were performed with *ASCA*. Our far-ultraviolet spectra cover the spectral range 820–1840 Å with a resolution of 2–4 Å. No significant variations were found between the two observations. The total spectrum, shown in Figure 2, has a red continuum, $f_\nu \sim \nu^{-1.89}$, with an observed flux of $2.2 \times 10^{-14} \text{ erg cm}^{-2} \text{ s}^{-1} \text{ Å}^{-1}$ at 1450 Å, slightly above the historical mean. Intrinsic absorption

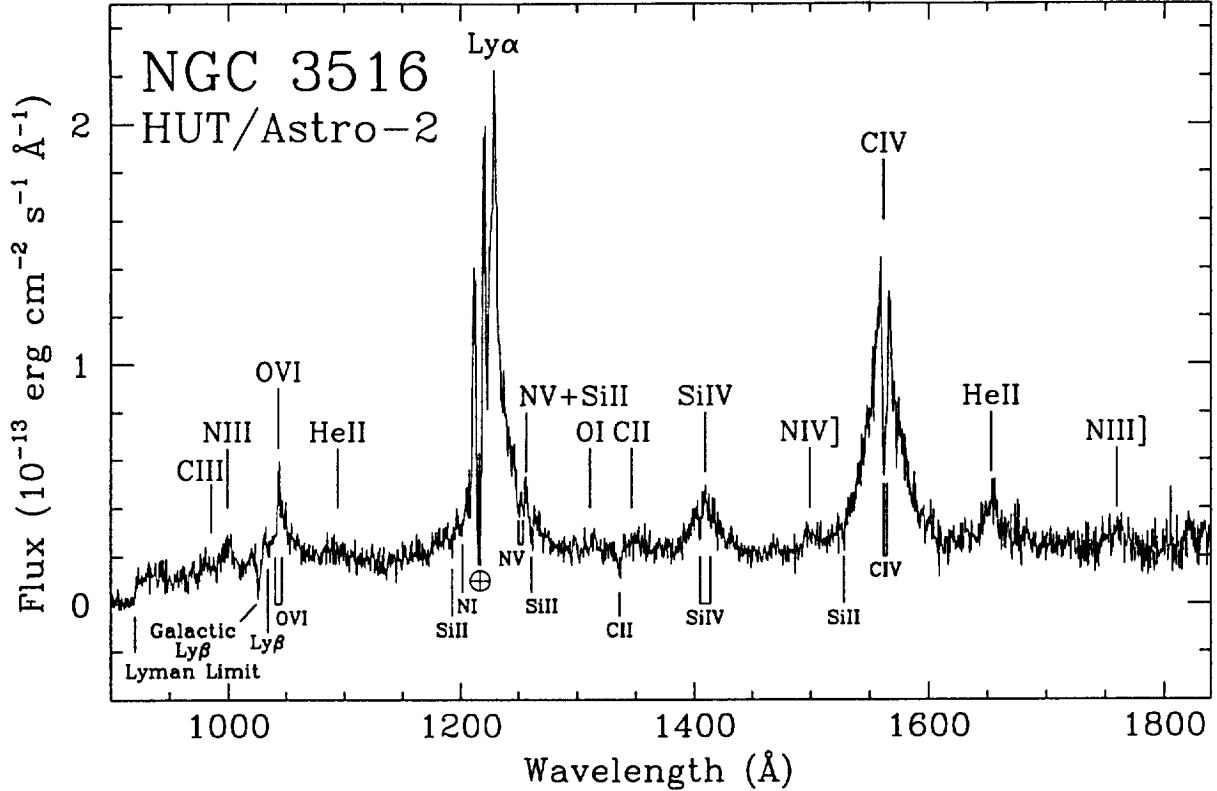


Figure 2: The flux-calibrated spectrum of NGC 3516 obtained with the Hopkins Ultraviolet Telescope during the Astro-2 mission is shown. Significant emission and absorption lines are marked. The indicated Lyman limit is at a redshift of 0.0075, and it is intrinsic to NGC 3516 as are the absorption lines of O VI, N V, Si IV, and C IV. The remaining absorption lines are likely galactic in origin. The earth symbol indicates the residual feature produced by subtraction of geocoronal Ly α emission.

in Lyman β is visible as well as absorption from O VI $\lambda\lambda 1032, 1038$, N V $\lambda\lambda 1239, 1243$, Si IV $\lambda\lambda 1394, 1403$, and C IV $\lambda\lambda 1548, 1551$. The UV absorption lines are far weaker than is usual for NGC 3516, and also lie closer to the emission line redshift rather than showing the blueshift typical of these lines when they are strong. The neutral hydrogen absorption, however, is blueshifted by 400 km s^{-1} relative to the systemic velocity, and it is opaque at the Lyman limit. The sharpness of the cutoff indicates a low effective Doppler parameter, $b < 20 \text{ km s}^{-1}$. For $b = 10 \text{ km s}^{-1}$ the derived intrinsic column is $3.5 \times 10^{17} \text{ cm}^{-2}$.

The ASCA spectrum (Figure 3) shows a lightly absorbed power law of energy index 0.78. The low energy absorbing column is significantly less than previously seen. Prominent O VII and O VIII absorption edges are visible, but, consistent with the much lower total absorbing column, no Fe K absorption edge is detectable. A weak, narrow Fe K α emission line from cold material is present as well as a broad Fe K α line. These features are similar to those reported in other Seyfert 1 galaxies.

A single warm absorber model similar to those calculated by Krolik & Kriss (1995) provides only an imperfect description of the low energy absorption. In addition to a highly ionized absorber with ionization parameter $U = 1.66$ and a total column density of $1.4 \times 10^{22} \text{ cm}^{-2}$, adding a lower ionization absorber with $U = 0.32$ and a total column of $6.9 \times 10^{21} \text{ cm}^{-2}$ significantly improves the fit. The contribution of resonant line scattering to our warm absorber models limits the Doppler parameter to $< 160 \text{ km s}^{-1}$ at 90% confidence. Turbulence at the sound speed of the photoionized

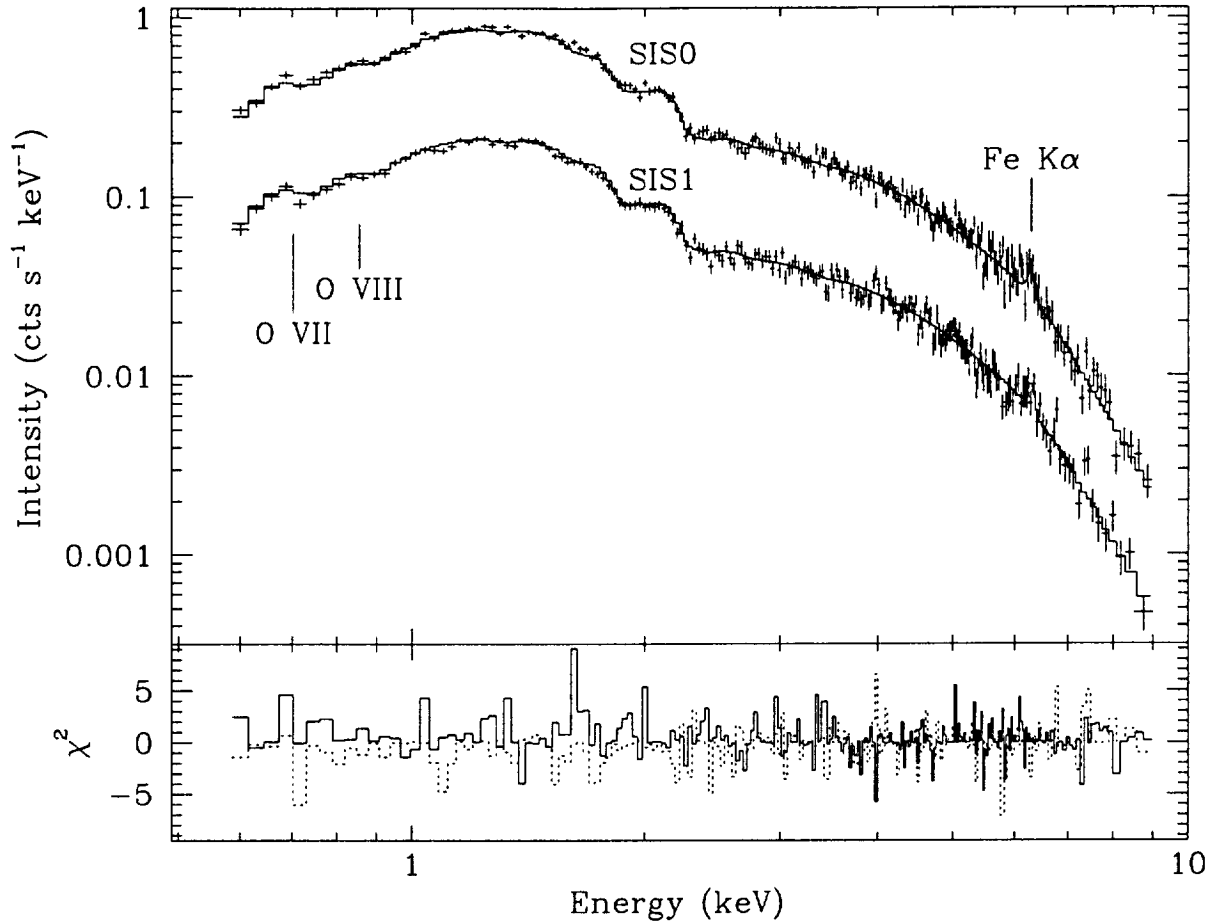


Figure 3. Kriss et al., ASCA Obs of NGC 3516. n3516x3.ps

Figure 3: *Upper Panel:* The solid lines are the best-fit empirical model folded through the ASCA SIS0 and SIS1 detector responses. The data points are crosses with 1σ error bars. The SIS1 data are offset down by 0.5 in the log for clarity. The model includes a power law with photon index 1.78, absorption by neutral gas with an equivalent neutral hydrogen column of $N_H = 6.8 \times 10^{20} \text{ cm}^{-2}$, a photoionization edge due to O VII at 0.71 keV with an optical depth at the edge of 0.65, a photoionization edge due to O VIII at 0.86 keV with optical depth 0.31, an unresolved iron $K\alpha$ line at 6.29 keV with an equivalent width of 73 eV, and a broad (FWHM = 1.58 keV) iron $K\alpha$ line at 5.88 keV with an equivalent width of 180 eV. *Lower Panel:* The contributions to χ^2 of each spectral bin are shown. The solid line is for SIS0 and the dotted line for SIS1.

gas provides the best fit. As in our observations of NGC 4151 (Kriss et al. 1995), a single warm absorber cannot produce the strong absorption visible over the wide range of observed ionization states. None of the warm absorber models fit to the X-ray spectrum can match the observed equivalent widths of all the UV absorption lines. Quantitatively, this is illustrated in Figure 4, where we plot the observed equivalent widths on curves of growth using the column densities predicted by the warm absorber models. Matching both the UV and X-ray absorption simultaneously requires absorbers spanning a range of 10^3 in both ionization parameter and column density.

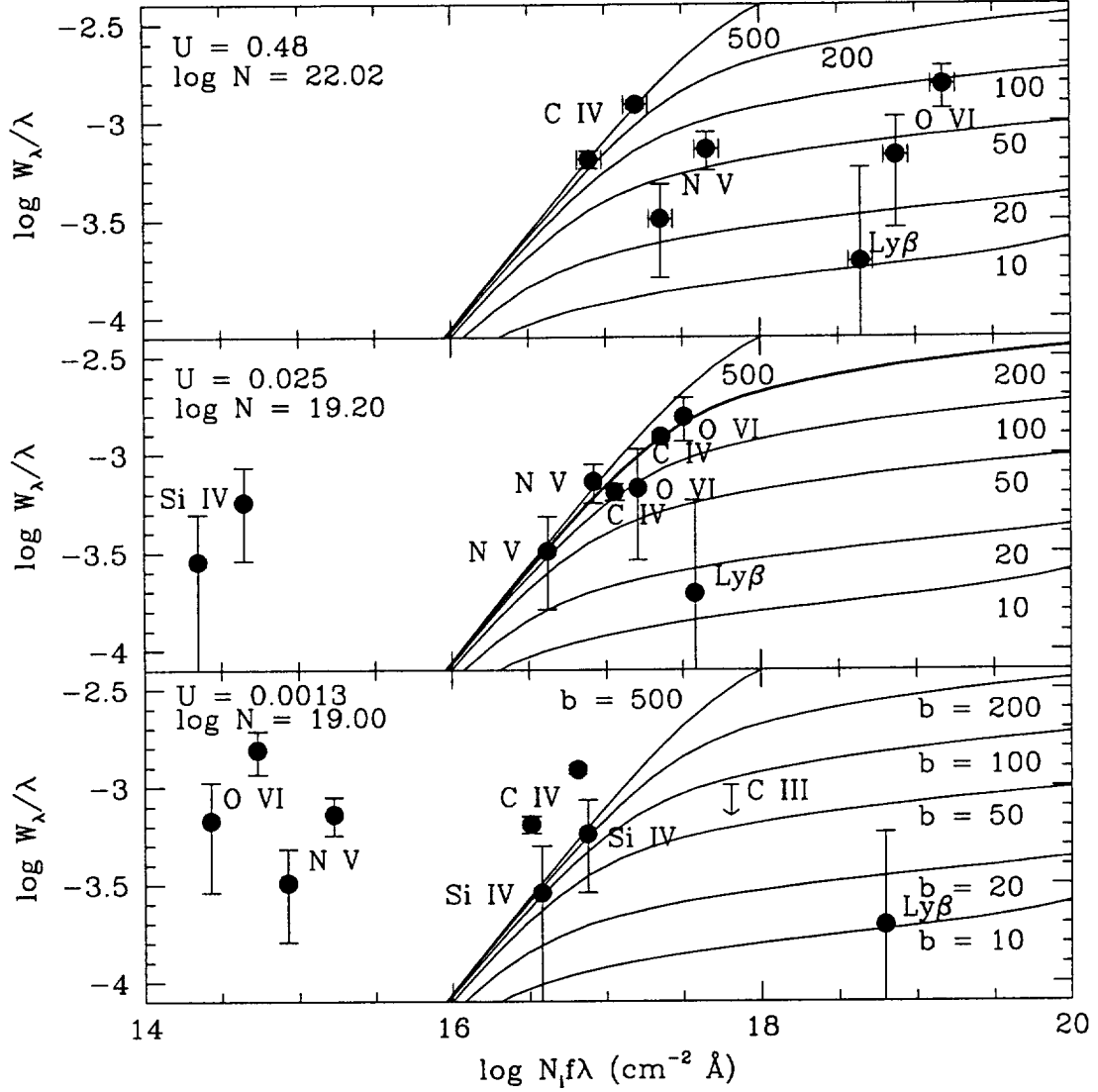


Figure 4: Kriew et al., MUF Obs of NGC 3516, n3516uv4.ps

Figure 4: *Top Panel:* The observed EWs of the UV absorption lines in NGC 3516 are plotted on curves of growth using column densities predicted by the single warm absorber fit to the ASCA X-ray spectrum. This model has $U = 0.48$ and a total column density of $10^{22.02} \text{ cm}^{-2}$. Points are plotted at a horizontal position determined by the column density for the given ion in the model with a vertical coordinate determined by the observed EW for the corresponding absorption line. The predicted column of Si IV in this model is too low to appear on the plot. The thin solid lines show predicted EWs as a function of column density for Voigt profiles with Doppler parameters of $b = 10, 20, 50, 100, 200$, and 500 km s^{-1} . A model that fits the data would have all points lying on one of these curves. This model cannot simultaneously match both the UV and the X-ray absorption. *Center Panel:* The observed EWs are plotted for column densities predicted by a model with $U = 0.025$ and a total column density of $10^{19.2} \text{ cm}^{-2}$. The heavy solid curve at $b = 200 \text{ km s}^{-1}$ gives a good match to the observed EWs of the C IV, N V, and O VI doublets, but the predicted EW of Si IV is far below the observed value. *Bottom Panel:* The observed EWs are plotted for column densities predicted by a model with $U = 0.0013$ and $N = 10^{19.0} \text{ cm}^{-2}$. $b = 20 \text{ km s}^{-1}$ can match the observed EWs of Si IV and Ly β and satisfy the upper limit on the EW of C III $\lambda 977$.

2.3 Small-Aperture Spectroscopy of the Gas Disk in M87

One of the initial incentives for our long-term program to study the structure of active galactic nuclei was the ability of the newly repaired HST to resolve a disk of ionized gas at the center of the giant elliptical galaxy M87 (Ford et al. 1994) and to measure the mass of the central black hole in this active galaxy using spatially resolved spectra to measure Keplerian rotational velocities in the disk (Harms et al. 1994). To improve upon these initial measurements we have made additional observations with smaller apertures at locations in the disk closer to the central black hole and at two positions out of the plane of the disk along the direction of the jet. The locations used for the small $0.086''$ aperture positions in the disk and the $0.26''$ aperture locations out of the disk plane are shown in Figure 5a.

Multiple components are apparent in the spectra shown in Figure 5b. Some of these we identify as outflowing gas along the radio jet. The remaining peaks extend our initial Keplerian rotation curve even closer in to the central black hole. Figure 6 shows the newly measured velocities along with those from Harms et al. (1994) fit to a Keplerian rotation curve projected onto our line of sight. The slope of the fit gives the mass of the central black hole. Preliminary fit parameters for the disk are an inclination $i = 36^\circ$, the line of nodes at $\theta = 6^\circ$, and a central black hole mass of $\sim 2 \times 10^9 M_\odot$. These all agree with our previous work, but our four closest points to the center of M87 now extend our measurements in to a mean radius of 6 pc. Estimating the stellar light interior to this radius from the photometry of Lauer et al. (1992), we obtain a preliminary mass-to-light

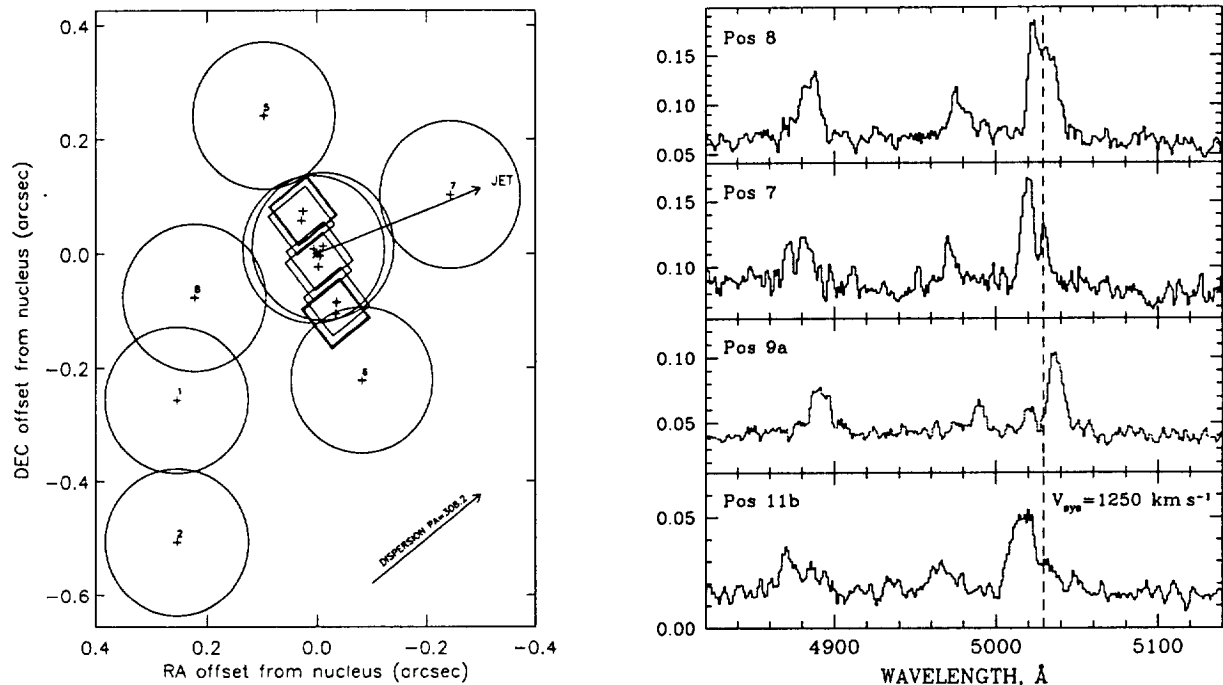


Figure 5: The left panel shows a schematic of the FOS aperture positions relative to the nucleus and the jet in M87. The small $0.86''$ square aperture observations were made at two different epochs at each position, accounting for the small differences in centering. The right panel shows representative FOS spectra at four positions in the center of M87. The vertical scale is in counts per second.

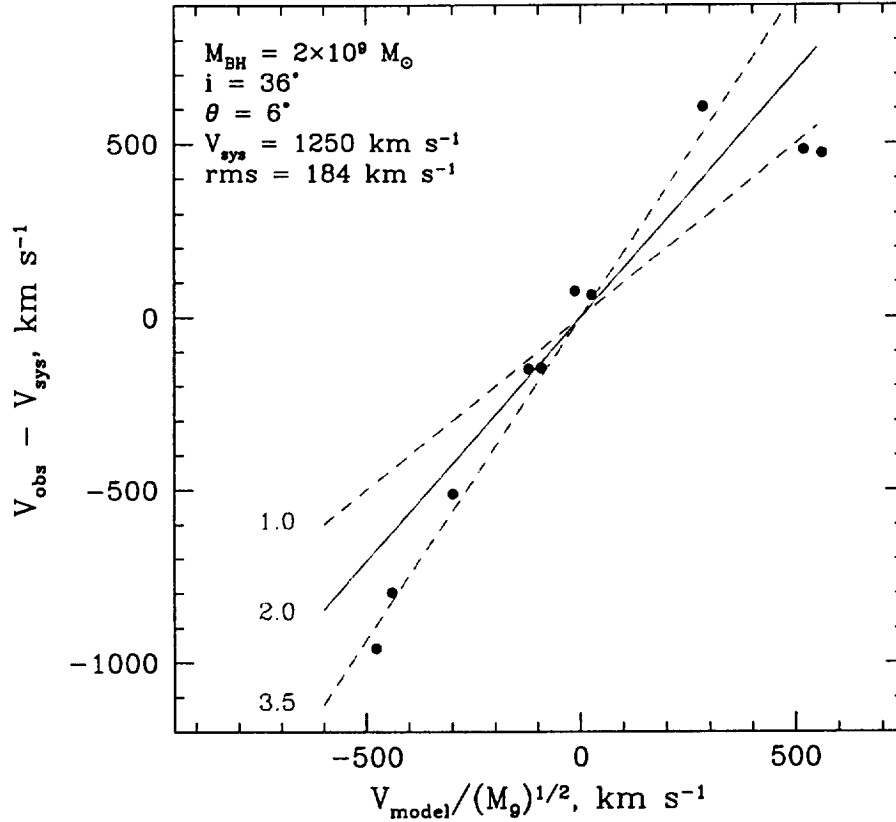


Figure 6: A preliminary fit of the velocities from Harms et al. (1994) along with our newly determined [O III] velocities to the projection of a Keplerian disk onto the line of sight. The slope gives the mass in units of $10^9 M_{\odot}$. The dashed lines are the extremes that bound the data between 1.0 and $3.5 \times 10^9 M_{\odot}$.

ratio of $(M/L)_V \sim 3000$. Given the goodness of the fit and the fact that the mass-to-light ratio continues to rise toward the center of M87, we again conclude that the active nucleus harbors a massive black hole.

2.4 Radio Observations of Southern Seyfert Galaxies

There are basically two types of collimated radiation observed in AGN — *radio jets* with typical opening angles of a few degrees, and *ionization cones* with characteristic opening angles of order a hundred degrees. The available data (Wilson & Tsvetanov 1994) show that the extended radio emission (jet) is *invariably* co-aligned with the ionization cone axis. We note that in the unified model the ionization cones result from shadowing of the nucleus by an optically thick parsec-scale torus. However, observations (and most theoretical analyses) suggest that the radio ejecta are collimated on a much smaller scale, possibly as small as the accretion disk. The observed tight alignment implies that radio plasma and ionizing photons are collimated by the same or strictly co-planar structures and there is no significant relative precession. Similarly, the radio jets are perpendicular to the even larger scale (~ 100 pc) nuclear disks like the ones observed with the HST in M87 (Ford et al. 1994) and NGC4261 (Jaffe et al. 1993).

On the arcsec or sub-arcsec scale the situation seems to be more complicated. High resolution

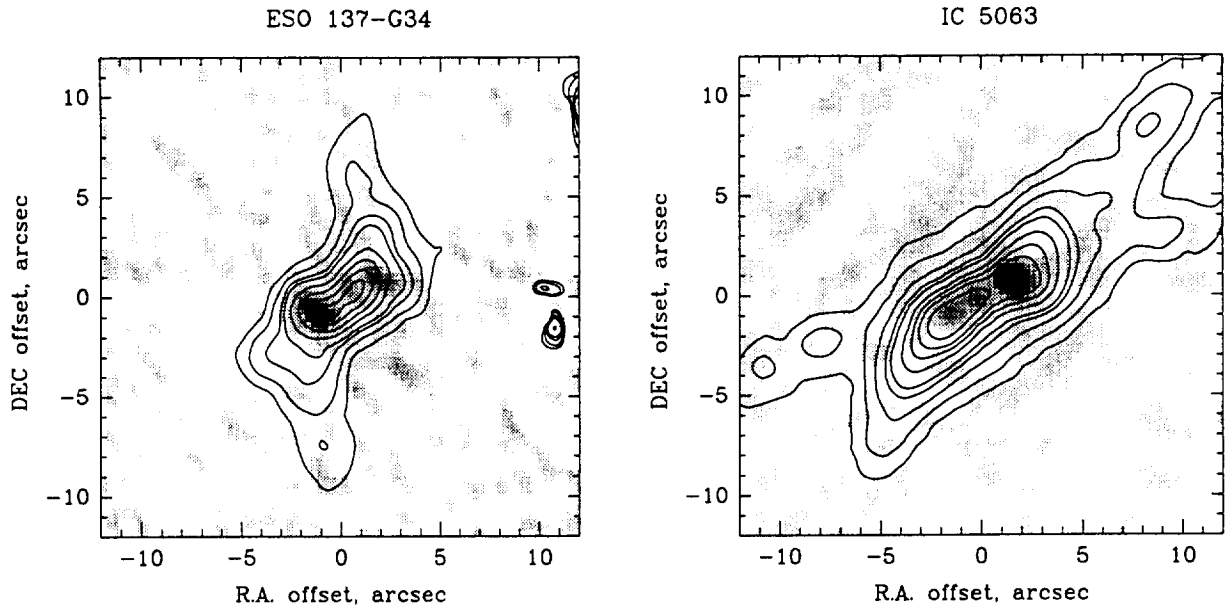


Figure 7: The left panel shows radio emission in ESO 137-G34 (grayscale) with contours of the [O III] $\lambda 5007$ line emission overlayed. The right panel shows a grayscale image of the radio emission in PKS 2048-57 (IC 5063) compared to the [O III] $\lambda 5007$ line emission contours.

images (many of them from HST) suggest a more complicated relationship between the radio and optical emission line with a very nice close correspondence observed in some cases and very little correspondence in some others. These results are mainly derived from observations of the most spectacular objects while to draw some statistical conclusions a well-defined sample with optical and radio data matching in resolution is required.

Recently we have completed an extensive emission-line imaging survey of a volume limited sample of southern Seyfert galaxies (Tsvetanov, Fosbury & Tadhunter 1996). This has provided high quality emission-line maps (in [OIII] $\lambda 5007$ and $H\alpha + [NII]$) with a typical resolution of $\sim 1''$ for a sample of 50 well-classified Seyferts south of declination 0° with $cz < 3600 \text{ km s}^{-1}$.

The most southern part of this sample ($\delta < -30^\circ$) has been observed at 8 GHz with the Australia Telescope Compact Array (ATCA) in the 6-km configuration. The resolutions of the obtained radio images is comparable with that of the optical images. For the northern part of the sample, snapshot observations were obtained earlier with the VLA at 6 cm. Of the 22 objects observed with the Compact Array (18 Seyfert Type 2 and 4 Type 1) only two are undetected. About half of the objects have an extended or slightly resolved radio emission. We also find that the objects with extended ionized gas tend to have a higher percentage of extended radio emission (compared to the objects where the ionized gas is restricted to the nucleus). The statistical significance of this difference, however, needs to be tested further.

A preliminary radio/optical comparison for the two objects with the strongest extended radio emission are very encouraging (Figure 7). In both ESO 137-G34 and PKS 2048-57 (IC 5063) a very good correspondence between the radio and emission-line morphologies is evident. This result supports the idea that, at least in some objects, interaction between the radio plasma and the warm gas is important on the arcsec and sub-arcsec scale. Shocks driven by the radio plasma are likely to be produced because of this interaction. The significance of these shocks for the overall energetics is,

however, an open question. Preliminary calculations on the energy budget in PKS 2048-57 suggests that the energy supplied by the radio plasma is not enough to explain the energy radiated in the emission lines. If this is further confirmed it may support the idea of nuclear photoionization as the primary ionizing mechanism and the interaction with the radio plasma being mainly responsible for shaping the morphology of the line-emitting gas.

3 Proposals Submitted and Approved during the First Year

To perform the observations which will form the core of our future research, we successfully submitted a number of proposals. Their status is summarized here.

- 1. HST Survey of Radio Ellipticals for Nuclear Disks**
Investigators: Ford, Jaffe, Tsvetanov, Kriss, Harms, & Dressel
Status: In the scheduling process. No data taken.
- 2. Survey of Compact Nuclear Radio Sources for Nuclear Disks**
Investigators: Dressel, Harms, Ford, Tsvetanov, & Kriss
Status: 3 of 12 observations completed, remainder still being scheduled.
- 3. High-resolution IR imaging of Seyfert Nuclei**
Investigators: Tsvetanov & Kriss
Status: Observations with the IRTF scheduled for February 28 & 29, 1996.
- 4. HI observations of the Centres of Seyfert Galaxies**
Investigators: Oosterloo, Morganti, Tsvetanov, Allen on the Australian Telescope Compact Array.
Status: Time allocated for 31-Mar-96; preliminary data taken Dec 95.
- 5. Optical/Radio Interaction in the Seyfert Galaxy PKS 2048-56**
Investigators: Morganti et al. on the Australian Long-Baseline Array.
Status: Scheduling is in progress.

4 Outlook for the Upcoming Year

The broad basis for our work will begin with these imaging surveys using HST and ground-based facilities. Due to the large amounts of requested observing time and scheduling practicalities, these observations will start this year and span several years. As the data become available, we will begin to define the samples for our followup imaging in other narrow band-passes and for our spectroscopic studies of resolved structure and UV and X-ray absorption. These will begin to some extent in the second year, but the bulk of the spectra are likely to be obtained in years three through five after the imaging surveys are completed. Analysis of the results will be contemporaneous with the observations and data reduction, but the comprehensive synthesis of the full data set will come in the final year of the program.

5 Publications in Year 1

1. "The Far-Ultraviolet Spectrum of NGC 4151 as Observed with the Hopkins Ultraviolet Telescope on the Astro-2 Mission", Kriss, G. A., Davidsen, A. F., Zheng, W., Kruk, J. W., & Espey, B. R. 1995, ApJ, 454, L7.
2. "HST FOS/COSTAR Small Aperture Spectroscopy of the Disk of Ionized Gas in M87", Ford, H., Tsvetanov, Z., Hartig, G., Kriss, G., Harms, R., & Dressel, L. 1996, in Science with the Hubble Space Telescope-II, eds. Benvenuti, P., Macchetto, F. D., & Schreier, E. J., (Space Telescope Science Institute: Baltimore), in press
3. "ASCA Observations of the Composite Warm Absorber in NGC 3516", Kriss, G. A., Krolik, J. H., Otani, C., Espey, B. R., Turner, T. J., Kii, T., Tsvetanov, Z., Takahashi, T., Davidsen, A. F., Tashiro, M., Zheng, W., Murakami, S., Petre, R., & Mihara, T. 1996, ApJ, submitted
4. "Far-Ultraviolet Observations of NGC 3516 using the Hopkins Ultraviolet Telescope", Kriss, G. A., Espey, B. R., Krolik, J. H., Tsvetanov, Z., Zheng, W., & Davidsen, A. F. 1996, ApJ, submitted
5. "Radio Continuum Morphology of Southern Seyfert Galaxies", Morganti, R., Tsvetanov, Z., Gallimore, J., Allen, M., & Caganoff, S. 1996, in preparation

6 References

- Ford, H. C., Harms, R. J., Tsvetanov, Z. I., Hartig, G. F., Dressel, L. L., Kriss, G. A., Davidsen, A. F., Bohlin, R., & Margon, B. 1994, ApJ, 435, L27
- Harms, R., Ford, H. C., Tsvetanov, Z., Hartig, G., Dressel, L., Bohlin, R., Kriss, G., Davidsen, A., Margon, B., & Kochhar, A. 1994, ApJ, 435, L35
- Jaffe, W., Ford, H. C., Ferrarese, L., van den Bosch, F., & O'Connell, R. W. O. 1993, Nature, 364, 213
- Kriss, G. A., Davidsen, A. F., Zheng, W., Kruk, J. W., & Espey, B. R. 1995, ApJ, 454, L7
- Kriss, G. A., et al. 1992, ApJ, 392, 485
- Krolik, J. H., & Kriss, G. A. 1995, ApJ, 447, 512
- Lauer, T. R., et al. 1992, AJ, 89, 1816
- Tsvetanov, Z., Fosbury, R., & Tadhunter, C. 1996, in preparation
- Wilson, A. S., & Tsvetanov, Z. I. 1994, AJ, 1227

7 Revised Budget and Cost Plan for Year 2

The peer review committee recommended personnel support as described below with a funding level of \$74,700 for the second year of our program. Our revised budget, using current salary figures, is slightly in excess of this original baseline. Drs. Kriss and Tsvetanov are funded at a level of two months per year for the life of the project, and Dr. Zheng is funded at 1 month per year. The senior investigators, Drs. Ford and Davidsen, are not funded. One month per year of secretarial support provides routine administrative assistance: typing, word processing, message center, copying, etc. JHU projects a personnel benefit rate of 29% for staff in UFY '96 (7/1/95 – 6/30/96) and a rate of 28% in UFY '97. A detailed breakdown of the individual entries in our budget summary is described here and in the accompanying table.

Consistent with the funding recommendations of the peer review, our travel costs include one observing trip per year each to Arizona and to Chile, one trip per year to an AAS meeting, and one trip per year to an international conference. For each five-day observing trip in Arizona we estimate costs at \$964 for round trip airfare, \$60/day lodging, and \$40/day meals and miscellaneous expenses. For each seven-day trip to Chile we estimate round-trip air fare at \$1850 and meals and lodging at \$100/day. For each five-day AAS trip we estimate costs at \$750 for round trip airfare, \$150 registration, \$80/day lodging, and \$40/day meals and miscellaneous expenses. For trips to an international conference we estimate seven-day trips with \$1,500 for round-trip air fare and \$200/day for meals and lodging.

Supplies and materials are the normal office type expended in this type of program, including magnetic tapes for data backup and storage, paper and toner for photocopying and laser printer output, and reference materials.

The Johns Hopkins Department of Physics and Astronomy has established a computing center with file servers to serve as boot nodes for workstations, to supply peripherals such as magnetic tape drives and laser printers, to negotiate group maintenance contracts, and to provide the services of a systems manager. Large software packages and software libraries such as IRAF are maintained on the file server. The center also maintains the network throughout the department. To partially defray the costs of providing these services, individual workstations are charged a monthly fee for access to the department network. This is anticipated to be \$15/month for UFY '97. Users are also charged a flat monthly fee of \$15/month for account maintenance. Hardware maintenance fees are \$72.20/month under the group contract with Sun Microsystems, and the annual software maintenance fee is \$125 for each operating system. During each year of the project we have charged these fees in direct proportion to the man-months of effort devoted to our study.

Publication costs cover the charges to print the results in *The Astrophysical Journal* and to distribute preprints. We include funds for two ApJ Letters in each of the first two years, and one 7–8 page ApJ article. Preprint costs are estimated at \$150/letter and \$250 per paper. It is anticipated that the number of publications will increase to three letters per year and articles of 7–13 pages in length in years 3–5.

For UFY 1996–1999 Johns Hopkins University has negotiated an IDC rate of 68%. The program will be charged the applicable rates in effect in later years. All numbers after 1997 are estimates, based on an annual inflation rate of 3%.